

Subsurface oscillations at an oceanic station in the Bay of Bengal

Y V B Sarma, M S S Sarma, R J Krishnamacharyulu & D P Rao

Physical Oceanography Division, National Institute of Oceanography, Dona Paula, Goa 403 004, India

Received 27 February 1990; revised 24 April 1991

Surface wind, atmospheric pressure and the temperature profiles in the upper layers at an oceanic station off west of Andaman Island in the Bay of Bengal have been analysed to examine the causes for the observed subsurface oscillations. For this purpose a 7 day time series data on water temperature, surface wind and atmospheric pressure have been taken. Spectral analysis of the data shows that the fluctuations of pressure and wind have varied influence on the subsurface oscillations. However, in the semi-diurnal tidal frequency band, the atmospheric pressure and normal and tangential components of wind exhibit a good coherence while at other frequencies they exhibit differential influence. The effect of the atmospheric pressure and the normal component of wind is predominant at lower frequencies and the effect of the tangential component of wind is predominant at higher frequencies. However, influence of atmospheric pressure fluctuations is less pronounced as compared with that of wind.

Temperature oscillation in the upper layers of the ocean is a common phenomenon which has been observed at many geographical locations of the ocean. These oscillations can be due to a variety of atmospheric as well as oceanic triggering mechanisms¹⁻³. These oscillations can also be due to internal waves which occur in the subsurface layers which are stratified due to temperature and salinity variations. An excellent review of different mechanisms of internal wave generation is given by Roberts¹. Thus these subsurface oscillations represent a significant mechanism for the transport of momentum and energy within the ocean¹.

To date, only a few studies on this aspect in the Bay of Bengal are made^{4,5}. But these studies are made at the locations very near to the coast where the boundary and the topographic effects could be dominant. So far, there are no studies available on this aspect in the open waters of the Bay of Bengal. Hence, an attempt is made to examine the internal oscillations at a deep location (11°30'N, 91°E), which is far from the coastal boundaries (Fig. 1). The nearest land boundary, the west coast of Andaman Islands, is some 160 km away and the depth at the above location is 3300 m. Hence, the topographic and coastal boundary influence on the generation of the internal oscillations at this location can either be absent or be insignificant. Hence, these oscillations are examined in relation to local wind and atmospheric pressure fluctuations.

Materials and Methods

Hourly time-series data on water temperature up to 400 m depth have been collected for 7 days from 0700 hrs, 1 November to 0600 hrs, 8 November 1985, using a MICOM bathythermograph. The accuracy of the temperature sensor is $\pm 0.05^\circ\text{C}$. Simultaneously the data on surface wind and atmospheric pressure fields also have been collected. Spectral estimates have been computed using FFT method⁶. The fourier components are computed by

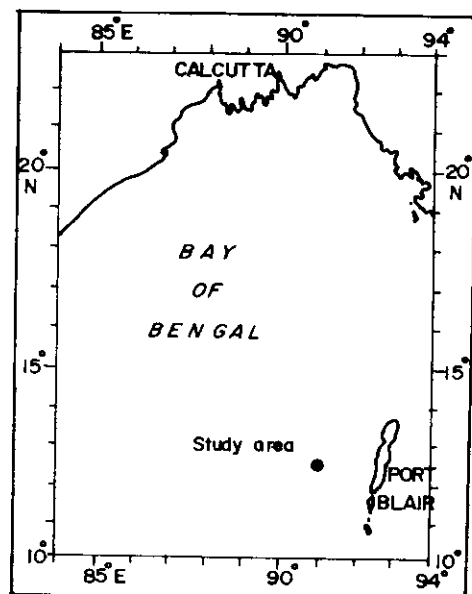


Fig. 1—Station location map

$$X_k = \sum_{n=0}^{N-1} x_n \exp\left(-i \frac{2\pi K \cdot n}{N}\right), \quad K = 0, 1, \dots, N-1$$

where, X = fourier component. Power spectral densities (PSDs) are given by

$$\frac{2\Delta T}{N \cdot S} |X_k|^2, \quad K = 0, 1, \dots, N/2$$

where S = scaling factor, N = number of data points, ΔT = sampling interval. PSDs correspond to the frequencies given by

$$f_k = \frac{k}{N \cdot \Delta T}, \quad k = 0, 1, \dots, N/2$$

The total length of the data has been divided into 4 segments with each segment having 40 data points. For each frequency an average PSD over all segments is obtained. The spectral estimates of water temperature, wind and atmospheric pressure have been made. In case of wind, the resolved components U (normal component) and V (tangential component) have been taken for the spectral analysis, where $U = W \sin \theta$ and $V = W \cos \theta$, W = the

unresolved magnitude of the scalar wind and θ = wind direction.

Results and Discussion

The thermal structure of upper 400 m depth is presented in Fig. 2. Sea surface temperature (SST) shows a mild drop with time and varies between 29.4° and 28.2°C during the observation period (Fig. 2A). The vertical time section of water temperature (Fig. 2B) shows that the subsurface oscillations are predominant in the lower thermocline region than in the upper thermocline region. In the upper 40 m water column the wavy pattern is absent due to turbulent mixing in the surface mixed layer. The magnitude of oscillation of different isotherms is not uniform throughout the water column. It is less in the upper thermocline region, where the vertical gradient of temperature is strong, and gradually increased towards bottom of the thermocline. The thermocline is located between 40 and 220 m depth. In the lower thermocline region, the magnitude of oscillation of the isotherms is as high as 30 m. Below the thermocline, the magnitude of oscillations is higher due to the weak stratification.

Power spectral estimates of the selected isotherms, wind components and pressure are shown

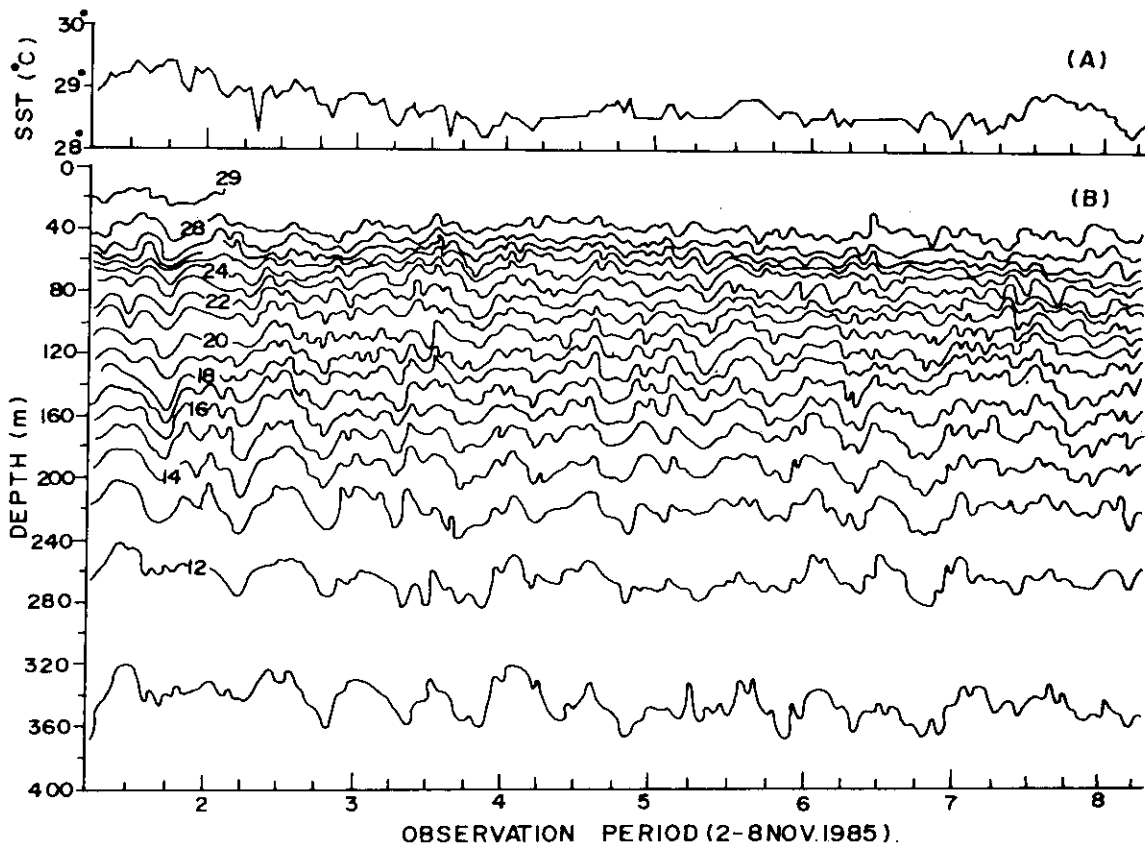


Fig. 2—Time section of—(A) sea surface temperature, (B) vertical distribution of temperature

in Fig. 3. In the present study 28°, 20° and 13°C isotherms have been chosen to represent top, middle and bottom regions of the thermocline respectively. Maximum spectral energy of the pressure is found

to be at 0.075 cph which is equivalent to the period of 13 h 20 min (Fig. 3A). Other notable peaks in the pressure spectrum are at 0.2, 0.275, 0.35 and 0.425 cph (ie, periods of 5 h, 3 h 35 min, 2 h 50 min and 2 h 15 min respectively). Normal as well as tangential components of wind have maximum energy at 0.025 cph which is equivalent to a period of 40 h (Fig. 3B,C). Wind components are stronger than the pressure in the semi-diurnal tidal frequency range. PSD of normal component of wind shows higher energies at lower frequencies. Spectral energies of tangential component are in general higher in the frequency range 0.075-0.3 cph compared to pressure and normal component of wind. The spectral density of 13°C isotherm (Fig. 3D) is higher than that of other 2 isotherms. All the 3 isotherms show maximum spectral density at 0.075 cph which includes semi-diurnal tidal period.

Coherence and phase of cross-spectral estimates of pressure, wind components and isotherms are shown in Fig. 4. The 28°C isotherm fluctuations show higher coherence with pressure and V-component at lower and higher frequencies (Fig. 4A,B). Whereas in intermediate range the coherence between 28°C and the forcing functions is in general < 0.3. Coherence between oscillations of 28°C and U-component of wind looks impressive only at a few frequencies in the lower frequency range. Maximum coherence with all the above parameters is seen at 10 h (5th lag). At tidal frequency, only pressure shows very good coherence with 28°C whereas, V-component shows very weak coherence. Coherence between V-component and 28°C is in general poor except at 0.025, 0.10 and 0.375 cph frequencies. Coherence of 20°C isotherm with pressure is

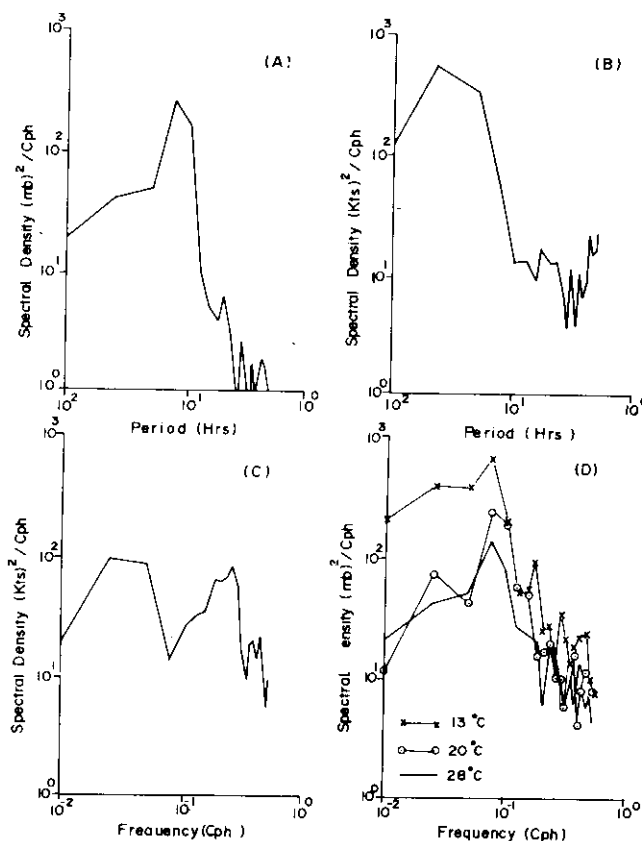


Fig. 3—Power spectra of—(A) pressure, (B) normal component of wind, (C) tangential component of wind, (D) 28°, 20°, 13°C isotherms

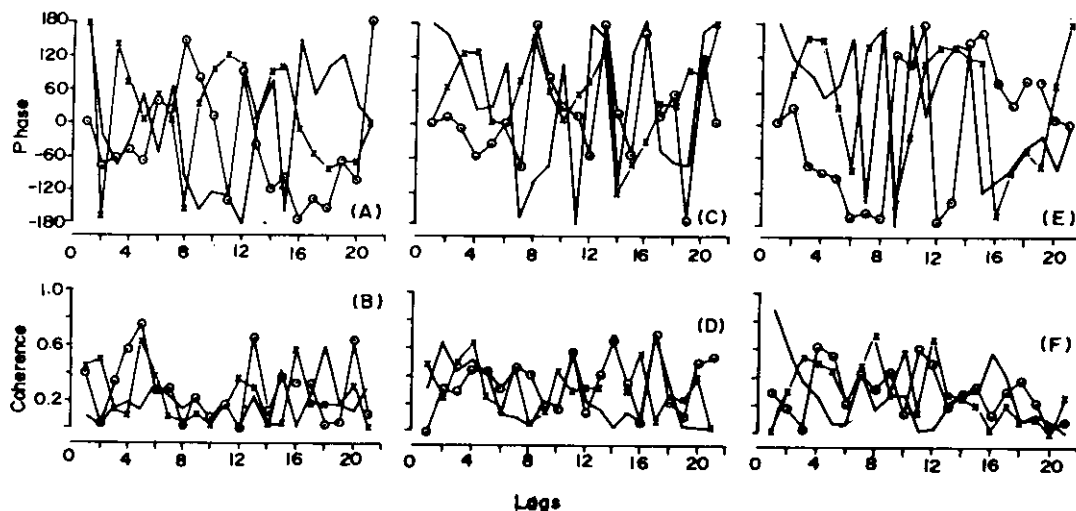


Fig. 4—(A,B) phase and coherence of 28°C isotherm with pressure (○—○), U-component of wind (×—×) and V-component of wind (●—●). (C,D) same as in (A,B) but for 20°C isotherm. (E,F) same as in (A,B) but for 13°C isotherm

low at lower frequencies including semi-diurnal tidal period (Fig. 4C,D). At tidal frequency the fluctuations in tangential component of wind are in weak coherence but in phase with 20°C isotherm whereas normal component of wind and pressure are 180° out of phase with 20°C isotherm. Coherence of normal component and 13°C is dominant compared with other 2 forcing functions (Fig. 4E,F). At higher frequencies the pressure and tangential component of wind exhibit one trend with 13°C and normal component of wind exhibits opposite trend.

Coherence and phase plots of cross-spectral estimates of the selected isotherms in the thermocline region are shown in Fig. 5. At tidal frequency good coherence and minimal phase difference are observed between all the isotherm. At 10 h (5th lag) also this trend is seen. Coherence between 20° and 13°C isotherms is always higher over all frequencies than that between 13°C and other isotherms. Higher phase differences are seen between 28°-20°C and 28°-13°C whereas, phase differences at different frequencies are relatively less between 20°-13°C isotherm oscillations. This indicates that the oscillations observed at the top of the thermocline are rather independent from the oscillations observed in the middle and at the bottom of the thermocline. At tidal frequency and also at 0.3 cph (about 3 h) the phase difference among different isotherms is very low.

In summary, the short period oscillations seem to be essentially generated and maintained by the fluctuations in the tangential component of wind. Long period oscillations are in good coherence with oscillations in atmospheric pressure and normal component of wind. At semi-diurnal tidal frequency pressure shows maximum energy whereas the normal component of wind has higher energy than the tangential component at the same frequency. Magnitude of oscillations of the isotherm increases with depth (Fig. 2). Cross-spectral estimates of different isotherms, which are in good coherence at the semi-diurnal tidal frequency, indicate the influence of the semi-diurnal tide up to deeper depths. At other frequencies, the oscillations of 28°C isotherm are different from the oscillations of 20° and 13°C isotherms. Influence of pressure and normal component of wind is dominant at lower frequencies

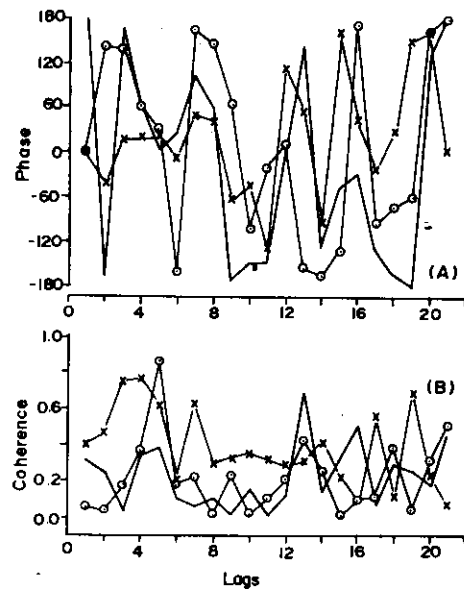


Fig. 5—Phase and coherence of selected isotherms 28°-20°C (●—●), 20°-13°C (×—×) and 13°-28°C (○—○)

whereas tangential component of wind exhibits good influence in the intermediate and higher frequency ranges. However, it would be difficult to determine the precise contribution of wind and pressure in causing the observed internal oscillations in the oceanic observations.

Acknowledgement

Authors express their gratitude to the Director and Dr. J.S. Sastry for their interest and support for this work. They also thank Mr. A.A. Fernandes and Mr. A.D. Gouveia for providing the computer program for spectral analysis.

References

- 1 Roberts J O, *Internal gravity waves in the ocean*, (Marcel Dekker Inc, New York) 1975, pp. 250.
- 2 Kase R H, *Dtsch Hydrogr Zeit*, 24 (1971) 193.
- 3 Krauss W, *Dtsch Hydrogr Zeit*, 25 (1972) 49.
- 4 Antony M K, Murty C S, Reddy G V & Rao K H, *Estuar Coast Shelf Sci*, 21 (1985) 823.
- 5 Sarma M S S & Rao L V G, *Mahasagar—Bull Natn Inst Oceanogr*, 22 (1988) 29.
- 6 Bendat J S & Piersol A G, *Random data analysis and measurement procedures*, (Wiley-Intersciences Inc, New York) 1972, pp. 388.